M2AN - MODÉLISATION MATHÉMATIQUE ET ANALYSE NUMÉRIQUE

MICHAL KOČVARA
MICHAEL ZIBULEVSKY
JOCHEM ZOWE

Mechanical design problems with unilateral contact

M2AN - Modélisation mathématique et analyse numérique, tome 32, n° 3 (1998), p. 255-281

<http://www.numdam.org/item?id=M2AN_1998__32_3_255_0>

MATHEMATICAL MODELLING AND NUMERICAL ANALYSIS
MODÉLISATION MATHEMATIQUE ET ANALYSE NUMERIQUE

(Vol 32, n° 3, 1998, p 255 à 282)

MECHANICAL DESIGN PROBLEMS WITH UNILATERAL CONTACT (*)

Michal KOČVARA (1), Michael ZIBULEVSKY (2) and Jochem ZOWE (1)

Abstract — *We formulate two problems of optimal design for mechanical structures in unilateral contact the truss topology problem and the material design problem for elastic bodies In both cases we consider general multi-load formulations, where for each load-case we may have different set of contact constraints (rigid obstacles) We show that both problems (after discretization of the latter one) can be rewritten as mathematical programs, which only differ in the character of the input data but otherwise have identical structure and thus allow the same algorithmic approach We propose an iterative optimization algorithm based on penalty-barrier methods A series of numerical examples demonstrates the usability and efficiency of our approach © Elsevier, Paris*

Résumé — *Nous formulons deux problèmes de conception optimale de structures mécaniques avec contacts unilatéraux topologie des armatures et distribution du matériau pour corps élastiques Pour ces deux problèmes, nous considérons des formulations générales multi-charges dans lesquelles les ensembles de contact peuvent être différents pour chaque cas de charge (obstacles rigides) Nous montrons que les deux problèmes (après discrétisation du second) peuvent être reformulés comme des problèmes d'optimisation qui ne diffèrent que par la nature des données mais de structure identique par ailleurs, ce qui permet le même traitement algorithmique Nous proposons un algorithme itératif utilisant les fonctions de pénalité-barrière. Une série d'exemples numériques témoigne de l'applicabilité et de l'efficacité de notre approche. © Elsevier, Paris*

1. INTRODUCTION

One of the basic problems of structural engineering reads: *For a given set of boundary conditions and a given set of loads, find the stiffest structure of a given volume that is able to carry the loads.* Very often, the boundary conditions are given by means of supports or obstacles with which the body is in *unilateral contact.* Such unilateral contact conditions introduce into the problem a new level of difficulty. In simple situations, when we can guess that the support "will be used", we can replace the contact condition by a standard (bilateral) boundary condition: we fix the respective nodes and thus simplify the problem. However, in many problems, in particular when the shape of the structure changes, the behaviour of the nodes or boundaries is unpredictable. Then we have to include the unilateral contact conditions into our model.

In this paper we study two variants of the above problem: a classical and a modern one. In the first variant, the structure to carry the loads consists of bars that are connected at joints (so-called truss). The design variables are the *bar volumes* and the goal is to choose the volumes (where the total volume is limited) such that the truss becomes as stiff as possible. In mathematical terms we maximize (with respect to bar volumes) the minimal (with respect to displacements) potential energy of the structure.

It is well-known that one can usually improve the optimal truss design by changing the position of the joints. To simulate also this aspect, we work with so-called *ground-structure* approach: We embed the truss into a dense mesh of potential bars and joints, which contains the starting layout and select from this fine mesh an optimal substructure. The price for this approach is the tremendous increase in the dimension of the problem. However,

(*) Manuscript received July 25, 1996 Revised November 13, 1996
Supported by the project 03ZO7BAY of the Federal Department of Education, Science, Research and Technology (BMBF), Germany, the EC grant CI1-CT92-0046, and the grant A1075707 of the Czech Academy of Sciences

(1) Institute of Applied Mathematics, University of Erlangen, Martensstr 3, 91058 Erlangen, Germany (kocvara@am uni-erlangen de and Zowe@am uni-erlangen.de)

(2) Faculty of Industrial Engineering, TECHNION—Israel Institute of Technology, Haifa 32000, Israel, (mcib@ie technion.ac il)

using the ideas introduced by Ben-Tal and Bendsøe [6] for the problems without contact, we can reformulate the problem as a linearly quadratically constrained program that can be efficiently solved by the powerful modified-barrier or interior-point methods introduced in [9], [17], see Section 4

In the second variant, the wanted structure is a two- or three-dimensional continuum elastic body The design variables are the *material properties* which, in this approach, may vary from point to point The objective is the same as in the first approach we maximize (with respect to material properties) the minimum potential energy, which characterizes the state of equilibrium for a given material under a given load The problem looks quite complicated at a first glance in two (three) dimensions, the design variables are the six (twenty one) elements of the symmetric elasticity tensor But we can analytically reduce it to a problem with only *one* design variable — the trace of the elasticity tensor, in analytical terms this corresponds to the bar volume in the first approach The elements of the optimal matrix are then fully recoverable from the optimal trace This idea goes back to Bendsøe *et al* [10] The reduced problem is discretized by the finite element method to get a mathematical program which is *identical* with that for the truss approach The only difference is in the character of the input data, namely geometry matrices of bars on one hand and finite element matrices on the other hand Hence the software developed for the truss approach can be almost immediately used in this framework of material optimization, with the only change in the input-data part

Let us emphasize that in our formulation of both problems and in the subsequent analysis, the contact conditions present no difficulty and introduce no additional work for the optimization algorithm

The truss topology problem with contact has been recently studied by Klarbring *et al* [18] and Peterson and Klarbring [23] The first paper, however, introduces one more design variable — the position of the obstacles and one more constraint — the sum of obstacle distances to the particular nodes should be zero This, although it seems to complicate it, enables to reduce the problem to a linear program Here we consider the position of the obstacles as input data (as well as other boundary conditions together with the magnitude and position of the forces) A polemic on the advantages and disadvantages of the two formulations is left to the reader The second paper [23] brings similar theoretical results as our Section 2 1 but does not include a numerical approach What we believe is essentially new in our approach is the treatment of the multi-load contact problem Moreover, we show that for each load-case we may define a different set of contact conditions (obstacles), covering thus very general scenarios

Petersson [21] and Petersson and Haslinger [22] have considered the continuum case, too However, they use the variable thickness approach (the material is given and the design variable is the thickness of a two-dimensional sheet) which usually leads to different designs (it is indeed a different problem), see Section 3 4 In our opinion, the variable thickness approach is less general in the context of topology optimization and has no counterpart in the three-dimensional space There are further approaches to the continuum problem, e g , the relaxation approach [4] or the homogenization method [11], see the introduction to Section 3 Our version has the advantage that it can be quite naturally generalized to contact problems, in particular, it is parallel to the truss topology problem, allowing us to apply our powerful numerical interior-point technique

2. THE DISCRETE CASE: TRUSS DESIGN

In this chapter we formulate and analyze the single- and multi-load problem of truss topology design based on the ground-structure approach The truss is in frictionless contact with a set of rigid obstacles We prefer to work with a saddle-point formulation for the potential energy For problems without contact, this formulation is equivalent to the minimum-compliance problem However, after introducing contact conditions, the two formulations are no longer equivalent and the minimum-compliance problem is almost impossible to solve numerically, whereas the 'potential energy' problem can be reformulated as a smooth convex optimization problem which is open to modern interior-point and penalty-barrier methods This reformulation has been recently introduced by Ben Tal and Bendsøe [6] (see also [19]) We will see that the contact conditions fit very naturally into this analysis and present no additional work for the numerical optimization algorithm

2.1. The single-load problem with contact: problem formulation

In *truss optimization* we want to design a pin-jointed framework (so-called *truss*) which is as stiff as possible under a given load f. The problem is modelled by a mesh of N tentative nodal points in $\mathbb{R}^{dim}$, where *dim* is 2 for planar and 3 for spatial trusses. Each two of these N nodes can be connected by a bar and thus we have $m = N(N-1)/2$ bars at our disposal, which are assumed to be slender and of constant mechanical properties characterized by their Young's moduli E_i, $i = 1, ..., m$. We consider the system under load, i.e., forces $f_j \in \mathbb{R}^{dim}$ are acting at some nodes j. They are aggregated in a vector f, where we put $f_j = 0$ for nodes that are not under load. This *external load* f is transmitted along the bars causing displacements of the nodes that make up the *state vector* u. Let p be the number of fixed nodal coordinates, i.e., the number of components with prescribed discrete homogeneous boundary condition. We omit these fixed components from the problem formulation reducing thus the dimension of u to

$$n = dim \cdot N - p \, .$$

Analogously, the external load f is considered as an element from $\mathbb{R}^n$.

The *design variables* in the system are the bar volumes $t_1, ..., t_m$ by which the designer can control the displacement vector u. To describe the interrelation between the t_i's (controls) and u_j's (state variables), we need the $n \times n$ *geometry-stiffness* matrix

$$A_i = \frac{E_i}{l_i^2} \gamma_i \gamma_i^T$$

of the i^{th} bar, where l_i is the length of this bar and γ_i the n-vector of direction cosines. The γ_i's locate the bars in the starting configuration and $\gamma_i^T u$ measures the bar elongation resulting from the displacement u. We work here in the framework of a linear theory. Hence, for a given volume vector

$$t := (t_1, ..., t_m)^T \geq 0_{\mathbb{R}^m} \quad (\text{i.e. } t_i \geq 0 \text{ for all } i) \, ,$$

the *assembled* $n \times n$ *stiffness matrix* of the system becomes

$$A(t) := \sum_{i=1}^{m} t_i A_i \, . \tag{2.1}$$

The matrix $A(t)$ is linear in t_i and E_i. Hence it is no restriction to assume from now on that $E_i = const$ for all i, since changes in E_i can be simulated by changes in t_i. This is in sharp contrast to the development in Chapter 3. For fixed t, the potential energy of the corresponding truss as a function of the displacement u is given by

$$\Pi_t(u) := \frac{1}{2} u^T A(t) \, u - f^T u \tag{2.2}$$

and the system is in equilibrium (i.e., the inner and the outer forces balance each other) for u which minimizes the potential energy

$$\min_{u \in \mathbb{R}^n} \Pi_t(u) \, . \tag{2.3}$$

As a nonnegative sum of dyadic products A_i, the matrix $A(t)$ is symmetric and positive semidefinite. Thus $\Pi_t(\,\cdot\,)$ is a convex function and the minimizers in (2.3) are characterized by the linear equality in u (*state equation*)

$$A(t) \, u = f \tag{2.4}$$

with the (negative) minimal value

$$\min_{u \in \mathbb{R}^n} \Pi_t(u) = \frac{1}{2} u^T A(t)\, u - f^T u_{|u\, A(t)\, u = f}$$

$$= -\frac{1}{2} f^T u_{|u\, A(t)\, u = f}. \tag{2.5}$$

The 'min' in (2.3) and (2.5) should be understood as $-\infty$ if (2.4) has no solution for the given t. Throughout we make the assumption

$$\text{linear hull of } \{\gamma_1, ..., \gamma_m\} = \mathbb{R}^n, \tag{2.6}$$

which ensures that

$$A(t) \text{ is positive definite for } t > 0 \quad (\text{i.e., } t_i > 0 \text{ for all } i). \tag{2.7}$$

Thus there are always values t for which (2.4) has a solution, i.e., the corresponding 'min' in (2.5) is a finite value.

The goal of the designer consists now in finding $t \geqslant 0$ under a volume constraint $\sum_{i=1}^{m} t_i = V$, for which the (negative) minimal potential energy becomes as large as possible. The resulting design problem reads as (we write $\Pi(t, u)$ instead of $\Pi_t(u)$ whenever we want to emphasise the role of t as a variable):

$$\max_{t \in T} \min_{u \in \mathbb{R}^n} \Pi(t, u), \tag{2.8}$$

where we put $T := \left\{ t \in \mathbb{R}^m \,|\, t \geqslant 0, \sum_{i=1}^{m} t_i = V \right\}$. In Section 2.2 we will see that assumption (2.6) ensures existence of 'max' and 'min' in (2.8) and below.

From (2.5) we get a reformulation of (2.8) (we skip a factor -1)

$$\min_{t \in \mathbb{R}^m,\, u \in \mathbb{R}^n} \left\{ \frac{1}{2} f^T u \,|\, t \geqslant 0, \sum_{i=1}^{m} t_i = V, A(t)\, u = f \right\}. \tag{2.9}$$

Version (2.9) is called *minimization of compliance* and is more popular than (2.8) in truss optimization. We will see, however, that in our context one should prefer (2.8) to (2.9).

The above objective of selecting an efficient bar system is called *topology optimization.* Version (2.8) is a max-min problem and the equivalent reformulation (2.9) suffers from nonconvex constraints $A(t)\, u = f$. Hence, straightforward numerical approaches do not seem to exist, neither to (2.8) nor to (2.9). What makes matters even worse is the fact that we would like to study (2.8) or (2.9), respectively, in the so-called *ground-structure* context. This technique aims at simulating additional 'moves' of the nodes (*geometry aspect*) by starting from an extremely dense mesh of tentative nodes and bars. Thus the dimensions n and m in (2.8) and (2.9) will be very high, typically n order $10^2 - 10^3$ and m even $10^3 - 10^5$. It is Carathéodory's theorem which ensures that the optimized truss gets along with only some few of the hundreds of potential nodes and ten thousands of potential bars; see, e.g. [19].

We now come to the central subject of this paper and suppose that some of the nodes have to stay within 'boxes' given by rigid obstacles. Such side conditions arise in a natural way in many engineering applications and are thus a 'must' for realistic modelling. We will treat such additional conditions in the framework of (2.8) and will only shortly touch the corresponding extension of (2.9) at the end of this section. The reason for this is twofold. First, such supplementary conditions perfectly fit into the max-min formulation (2.8), whereas they lead to clumsy additonal variables in (2.9). Second, and this is more important in this numerical paper: to the contact version of (2.8) we can directly apply the powerful modified-barrier and interior-point codes, which were recently developed for (a straightforward rephrasing of) (2.8) (see [9], [17]).

We study the case of frictionless and adhesionless unilateral contact coming from rigid obstacles associated with certain nodes. In mathematical language, the obstacles are given by linear inequalities stating that the displacements of the associated nodes cannot exceed given prescribed values in certain directions. Assume that, altogether, we have r conditions (nodal obstacles)

$$-v_i^T u \leqslant g_i, \quad i = 1, ..., r, \tag{2.10}$$

where v_i is the vector of direction cosines of the normal to the obstacle surface and $g_i \in \mathbb{R}$ is the distance of this surface to the associated node, see figure 1. We may have several obstacles for a particular node and allow the case of 'negative' distance g_i, i.e., the node is forced to move in the direction v_i by at least g_i. Some typical situations covered by our model are depicted in figure 2 (*fig.* 2(c) shows an example with negative g_i's).

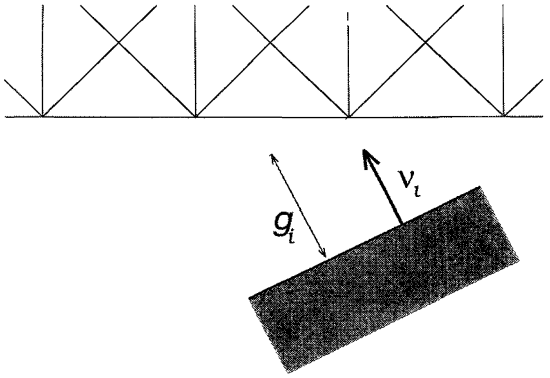

Figure 1. — Obstacle for the i-th node of a truss.

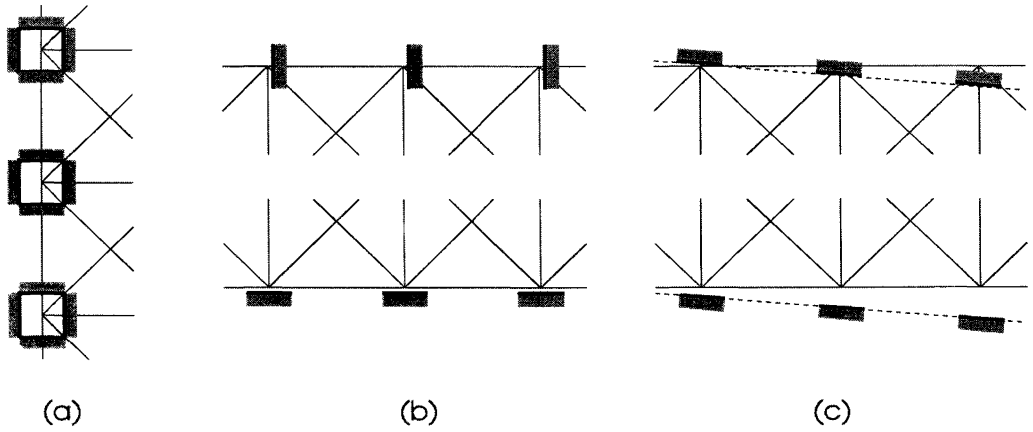

Figure 2. — Examples of different obstacles.

With the $r \times n$ matrix

$$C := -\begin{pmatrix} v_1^T \\ \vdots \\ v_r^T \end{pmatrix}$$

and the vector $g := (g_1, ..., g_r)^T \in \mathbb{R}^r$ we put

$$K := \{u \in \mathbb{R}^n \mid Cu \leqslant g\}. \tag{2.11}$$

This set has to be added as an additional constraint to (2.3), i.e., to the inner 'min' in (2.8):

$$\min_{u \in K} \Pi_t(u). \tag{2.12}$$

For given t, (2.12) characterizes the state of equilibrium of a truss in contact with an obstacle. Thus the design problem (2.8), enriched by contact conditions, becomes

$$\max_{t \in T} \min_{u \in K} \Pi(t, u). \tag{2.13}$$

Obviously, (2.12) and (2.13) only make sense for

$$K \neq \phi, \tag{2.14}$$

which we assume throughout the following. Problem (2.13) differs from (2.8) only by the additional linear constraint $Cu \leqslant g$ and it turns out that we can copy the technique, developed in [7], [19] for the contact-free problem (2.8), to prove existence of optimal solutions also for (2.13) and to derive an efficient code for computing optimal design vectors t. This will be done in the following.

We start with a simple reformulation which serves as a basis for our numerical approach. By a standard Minimax Theorem (see e.g. [27]), we may switch 'max' and 'min' in the concave-convex problem (2.13) and get

$$(2.13) = \min_{u \in K} \max_{t \in T} \Pi(t, u).$$

For each fixed u, the inner 'max' is a linear problem in t:

$$\max_{t \in T} \Pi(t, u) = \max_{t \in T} \left(\frac{V}{2} u^T A_1 u - f^T u, ..., \frac{V}{2} u^T A_m u - f^T u \right) \begin{pmatrix} t_1 \\ \vdots \\ t_m \end{pmatrix},$$

and thus, by LP-theory, only the extremal points $t = e_i \in \mathbb{R}^m (i = 1, ..., m)$ of the feasible set T play a role when minimizing over t. Hence (2.13) reduces to minimization of a finite max-function:

$$(2.13) = \min_{u \in K} F(u) \quad \text{with} \quad F(u) := \max_{1 \leqslant i \leqslant m} \left(\frac{V}{2} u^T A_i u - f^T u \right). \tag{2.15}$$

F is a nonsmooth convex function whose minimization requires special software. Such software exists and has been successfully applied in the truss context for moderate dimensions m and n ([3]). An approach, which can also deal with extremely large m and n, relies on a standard reformulation of (2.15) by adding an auxiliary variable α

$$(2.13) = \min_{\alpha \in \mathbb{R}, u \in \mathbb{R}^n} \left\{ \alpha - f^T u \mid Cu \leqslant g, \alpha \geqslant \frac{V}{2} u^T A_i u \text{ for } i = 1, ..., m \right\}. \tag{2.16}$$

The linearly-quadratically constrained problem (2.16) is open to the powerful modern modified-barrier methods and interior-point codes introduced in [9], [17]; see Section 4.

In Section 2.2 we will show that (2.16) always has an optimal solution (α^*, u^*) and that this u^* together with the Lagrange multiplier vector t^* of the quadratic constraints in (2.16) yields a solution of our original problem (2.13). We add that the mentioned modified-barrier and interior-point methods provide such t^* 'for free' when solving (2.16).

Let us come back to the point that, when adding contact conditions, we prefer the max-min formulation (2.8) to the equivalent min-compliance problem (2.9). As pendant to the optimality condition (2.4) for (2.3), we get for (2.12).

PROPOSITION 1: *The vector $u^* \in \mathbb{R}^n$ is a (global) optimal solution of (2.12) for given $t \geq 0$ if and only if there exists $p^* \in \mathbb{R}^r$ which together with u^* satisfies*

$$\left.\begin{aligned} Cu^* \leqslant g \quad \text{and} \quad p^* \leqslant 0 \\ A(t)\, u^* - f - C^T p^* = 0 \\ p^{*T}(Cu^* - g) = 0\,. \end{aligned}\right\} \tag{2.17}$$

Proof: For given $t \geq 0$ the minimization (2.12) is a convex quadratic problem in u and thus the Karush-Kuhn-Tucker conditions (2.17) are necessary and sufficient for the optimality of u^*. ■

The Lagrange-multiplier vector p^*, associated with the non-penetration constraint $Cu \leqslant g$ has a physical meaning: it is the reaction vector of the nodal contact forces and is not known *a priori.*

Using (2.17), the minimal value in (2.12) becomes

$$\min_{u \in K} \Pi_t(u) = \tfrac{1}{2} u^T A(t)\, u - f^T|_{u \text{ s t } (2\,17) \text{ holds}}$$

(and, after some simple arithmetic)

$$= \tfrac{1}{2} u^T (f + C^T p) - f^T u|_{u \text{ s t } (2\,17) \text{ holds}}$$

$$= -\tfrac{1}{2} f^T u + \tfrac{1}{2} u^T Cp|_{u \text{ s t } (2\,17) \text{ holds}}$$

$$= -\tfrac{1}{2} f^T u + \tfrac{1}{2} p^T g|_{u \text{ s t } (2\,17) \text{ holds}}\,. \tag{2.18}$$

By inserting (2.18) into (2.13) (just as (2.5) into (2.8)), we obtain as *minimal compliance* formulation for the problem with contact constraints (we skip again the factor -1)

$$\min_{t \in \mathbb{R}^m,\, u \in \mathbb{R}^n,\, p \in \mathbb{R}^r} \left\{ \tfrac{1}{2} f^T u - \tfrac{1}{2} g^T p \,|\, t \in T\,;\, u \text{ and } p \text{ s.t. } (2.17) \text{ holds} \right\}. \tag{2.19}$$

Note that (2.19) is a nonconvex problem which is almost impossible to solve numerically (in this formulation), even for small numbers n, m and r !

2.2. The single-load problem with contact: existence of solution

Recall our original problem (2.13) and its substitute (2.16)

$$\max_{t \in T} \min_{u \in K} \Pi(t, u) \quad \text{with} \quad \Pi(t, u) = \tfrac{1}{2} u^T A(t)\, u - f^T u \tag{2.20}$$

$$\min_{\alpha \in \mathbb{R},\, u \in \mathbb{R}^n} \left\{ \alpha - f^T u \,|\, \alpha \geqslant \frac{V}{2} u^T A_i\, u \text{ for } i = 1, \ldots, m, \text{ and } u \in K \right\}, \tag{2.21}$$

with the feasible sets

$$T = \left\{ t \in \mathbb{R}^m \mid t \geq 0, \sum_{i=1}^{m} t_i = V \right\}$$

$$K = \{ u \in \mathbb{R}^n \mid Cu \leq g \} .$$

The existence of an optimal solution for (2.20) is a direct consequence of a standard saddle-point theorem (see [27]).

THEOREM 2: *Problem (2.20) has an optimal solution* (t^*, u^*).

Theorem 2 together with the next statement implies that also (2.21) has an optimal solution.

THEOREM 3: *If* (t^*, u^*) *is a saddle-point for (2.20) then* (α^*, u^*) *with* $\alpha^* := \max_{1 \leq i \leq m} \frac{V}{2} u^T A_i u - f^T u$ *is an optimal solution to (2.21).*

Proof: From Section 2.1 we know that

$$\max_{t \in T} \min_{u \in K} \Pi(t, u) = \min_{\alpha \in \mathbb{R}, u \in \mathbb{R}^n} \left\{ \alpha - f^T u \mid \alpha \geq \frac{V}{2} u^T A_i u \text{ for } i = 1, ..., m, \text{ and } u \in K \right\} . \tag{2.22}$$

The claim follows easily from this. ■

In our numerical approach we will solve (2.21). The next result says how to recover a solution of our original problem (2.20) from the solution of (2.21).

THEOREM 4: *Suppose that* (α^*, u^*) *solves (2.21) with the multipliers* $\lambda^* \in \mathbb{R}^m$ *and* $p^* \in \mathbb{R}^r$ *for the quadratic and contact constraints, respectively. Put* $t^* := \lambda^* V$. *Then* (t^*, u^*) *is a saddle-point for* $\Pi(t, u)$, *i.e.,*

$$\Pi(t, u^*) \leq \Pi(t^*, u^*) \leq \Pi(t^*, u) \quad \text{for all } t \in T \text{ and } u \in K . \tag{2.23}$$

Proof: (2.21) is a convex problem and thus optimality of (α^*, u^*) is characterized by the Karush-Kuhn-Tucker conditions: there exists $\lambda^* \in \mathbb{R}^m$, $\lambda^* \geq 0$, and $p^* \in \mathbb{R}^r$, $p^* \leq 0$ such that

$$\sum_{i=1}^{m} \lambda_i^* = 1 \tag{i}$$

$$\frac{V}{2} A(\lambda^*) u^* - f - C^T p^* = 0 \tag{ii}$$

$$\lambda_i^* \left(\alpha^* - \frac{V}{2} u^{*T} A_i u^* \right) = 0 \quad \text{for } i = 1, ..., m \tag{iii}$$

$$p^{*T} (Cu^* - q) = 0 . \tag{iv}$$

From (i) and (iii) we get by summing up

$$\alpha^* - \frac{V}{2} u^{*T} A(\lambda^*) u^* = 0$$

and thus

$$\alpha^* - \frac{1}{2} u^{*T} A(t^*) u^* = 0 . \tag{2.24}$$

Now, for arbitrary $t \in T$, the feasibility $\alpha^* \geq \frac{V}{2} u^{*T} A_t u^*$ implies

$$\frac{t_i}{V}\left(\alpha^* - \frac{V}{2} u^{*T} A_t u^*\right) \geq 0 \quad \text{for } i = 1, ..., m$$

and, summing up again,

$$\alpha^* - \frac{1}{2} u^{*T} A(t)\, u^* \geq 0 .$$

This together with (2.24) shows

$$\Pi(t, u^*) \leq \Pi(t^*, u^*) \quad \text{for } t \in T .$$

To prove the right-hand side inequality in (2.23), note that (ii) and (iv) imply

$$\frac{1}{2} u^{*T} A(t^*)\, u^* - f^T u^* \leq \frac{1}{2} u^T A(t^*)\, u - f^T u \quad \text{for } u \in K$$

and thus

$$\Pi(t^*, u^*) \leq \Pi(t^*, u) \quad \text{for } u \in K .$$

■

2.3. The multi-load and 'multi-obstacle' problem

Let us now assume that we have several load cases and want to find the stiffest truss which can carry the different loads f_k, $k = 1, ..., M$. The development is analogous to the single-load case (it is just more technical), so we skip here the existence theorems and refer to the literature. As in the single-load case, we start with a non-standard formulation of the problem based on minimization of potential energy, show that it is equivalent to the classical 'minimum-compliance' formulation and then add the contact conditions.

First let us assume that we have a given volume vector

$$t := (t_1, ..., t_m)^T \geq 0_{\mathbb{R}^m}.$$

To each load f^k ($k = 1, ..., M$) there exists a displacement vector u^k (unique whenever $t > 0$), which minimizes the potential energy

$$\Pi_t^k(u^k) := \frac{1}{2} (u^k)^T A(t)\, u^k - (f^k)^T u^k . \tag{2.25}$$

Looking for a 'better' design vector t, we have to decide which load case is relevant with respect to the designer's point of view. A conservative way is to look for the so-called *worst case design* (*cf.*, e.g. [15]) where we consider the minimum of the potential energies over the load cases:

$$\min_{1 \leq k \leq M} \min_{u^k \in \mathbb{R}^n} \Pi_t^k(u^k) . \tag{2.26}$$

Now, analogously to the single-load case, we want to find $t \geq 0$ under a volume constraint $\sum_{i=1}^{m} t_i = V$, for which the minimal potential energy (2.26) is as close to zero as possible (*cf.* (2.8)):

$$\max_{t \in T} \min_{1 \leq k \leq M} \min_{u^k \in \mathbb{R}^n} \Pi^k(t, u^k) . \tag{2.27}$$

Again, using (2.5), we can rewrite (2.27) as

$$\min_{t\in T}\ \min_{1\leqslant k\leqslant M}\left\{\frac{1}{2}(f^k)^T u^k \mid t\geqslant 0,\ \sum_{i=1}^{m} t_i = V,\ A(t)\,u^k = f^k\right\}; \tag{2.28}$$

this is the standard minimum-compliance formulation of the multi-load problem (*cf.* Achtziger [1, 2]).

In order to get rid of the 'discrete' min-term in (2.27), we introduce the set

$$\Lambda := \left\{\lambda\in\mathbb{R}^M \mid \lambda_k\geqslant 0 \quad \text{for } k=1,\ldots,M,\ \sum_{k=1}^{M}\lambda_k = 1\right\}$$

and formulate (2.27) equivalently as

$$\max_{t\in T}\ \min_{\lambda\in\Lambda}\ \min_{u\in\mathbb{R}^{M\cdot n}}\left\{\sum_{k=1}^{M}\lambda_k\Big(\frac{V}{2}(u^k)^T A(t)\,u^k - (f^k)^T u^k\Big)\right\} \tag{2.29}$$

with the notation $u = ((u^1)^T, (u^2)^T, \ldots, (u^M)^T)^T\in\mathbb{R}^{M\cdot n}$. Now, analogously to (2.13), we can introduce the contact conditions $u^k\in K$ with K being defined in (2.11). Our approach allows us to deal with an interesting generalization by working with different constraint sets

$$K^k := \{u^k\in\mathbb{R}^n \mid C^k u^k\leqslant g^k\}$$

for different load-cases $k = 1, \ldots, M$. This means that for each load-case we may have a different set of obstacles. As a special case, we can consider a problem where all the loads are the same ($f^k = f$, $k = 1, \ldots, M$) but the sets K^k are different. In other words, we want to find the stiffest truss which is subject to one load but which, in different situations, has different obstacles.

The available scenarios are schematically depicted in figure 3: (a) presents a single-load case with one obstacle; (b) a scenario with two load-cases and one common obstacle; in (c) we have one load but two obstacles for two different situations and in (d) two load-cases with two different obstacles.

The combined multi-load & multi-obstacle problem analogous to (2.13) reads as:

$$\max_{t\in T}\ \min_{\lambda\in\Lambda}\ \min_{u\in K}\left\{\sum_{k=1}^{M}\lambda_k\Big(\frac{V}{2}(u^k)^T A(t)\,u^k - (f^k)^T u^k\Big)\right\} \tag{2.30}$$

with $K := K^1\times K^2\times\cdots\times K^M$. Copying steps which led from (2.13) to (2.15) we can rewrite (2.30) as a displacement-only problem (for technical details, see [1]):

$$\min_{\lambda\in\Lambda}\ \min_{u\in K}\ \max_{1\leqslant i\leqslant m}\left\{\sum_{k=1}^{M}\lambda_k\Big(\frac{V}{2}(u^k)^T A_i\,u^k - (f^k)^T u^k\Big)\right\}. \tag{2.31}$$

With the change of variables

$$s := \sqrt{\lambda},\quad v := \frac{u}{s}$$

we get a numerically more tractable problem

$$\min_{s\in S}\ \min_{v\in Q}\ \max_{1\leqslant i\leqslant m}\left\{\sum_{k=1}^{M}\Big(\frac{V}{2}(v^k)^T A_i\,v^k - s_k(f^k)^T v^k\Big)\right\} \tag{2.32}$$

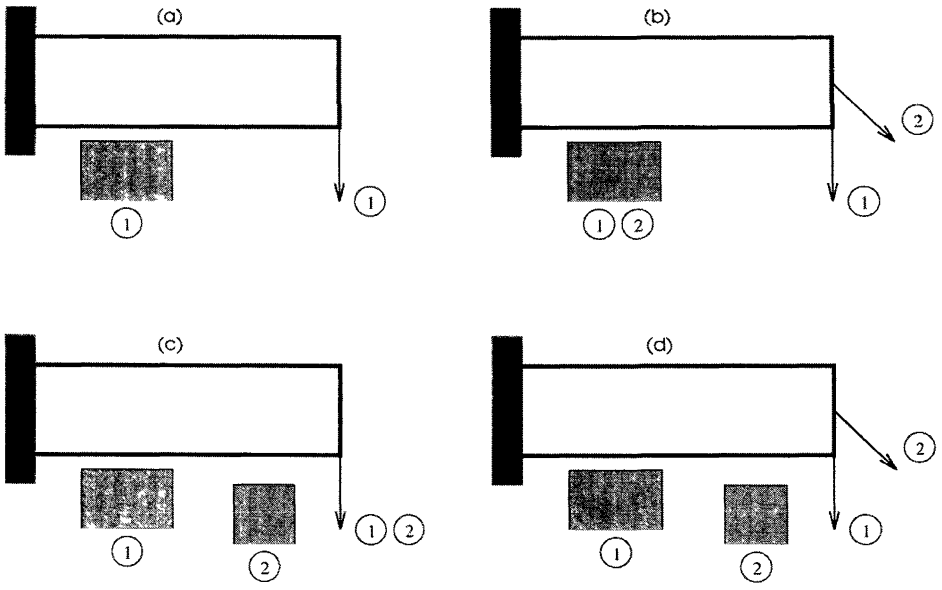

Figure 3. — Available scenarios for multi-load & multi-obstacle problems.

with the new feasible sets

$$S := \left\{ s \in \mathbb{R}^M \mid s_k \geq 0, \sum_{k=1}^{M} (s_k)^2 = 1 \right\}$$

$$Q := Q^1 \times Q^2 \times \cdots \times Q^M, \quad Q^k := \{ v \in \mathbb{R}^m \mid C^k v \leq s_k g^k \}, \quad k = 1, ..., M$$

according to the change of variables.

In the final step, we rewrite (2.32) as a smooth (but nonconvex) problem by adding an auxiliary variable α (*cf.* (2.16)):

$$\begin{aligned} \underset{s, v, \alpha}{\text{minimize}} \ \alpha - \sum_{k=1}^{M} s_k (f^k)^T v^k \text{ subject to } \quad & s \in S \\ & v^k \in Q^k, \quad k = 1, ..., M \\ & \frac{V}{2} \sum_{k=1}^{M} (v^k)^T A_i v^k - \alpha \leq 0, \quad i = 1, ..., m . \end{aligned} \tag{2.33}$$

2.4. Examples

In this section we present results of two numerical examples. The notation used in the pictures should be clear from figure 4.

Example 1: We consider a truss of length-height 10×1 with 17×7 nodes and 4322 tentative bars (each two nodes are connected by a bar). As shown in figure 5(e), the truss is supported from below at four points and is subject to two load-cases: the first one consists of forces applied at two upper corners, the second one of a force at the upper middle node. We could consider it to be a crane in a factory, moving on two pairs of rails.

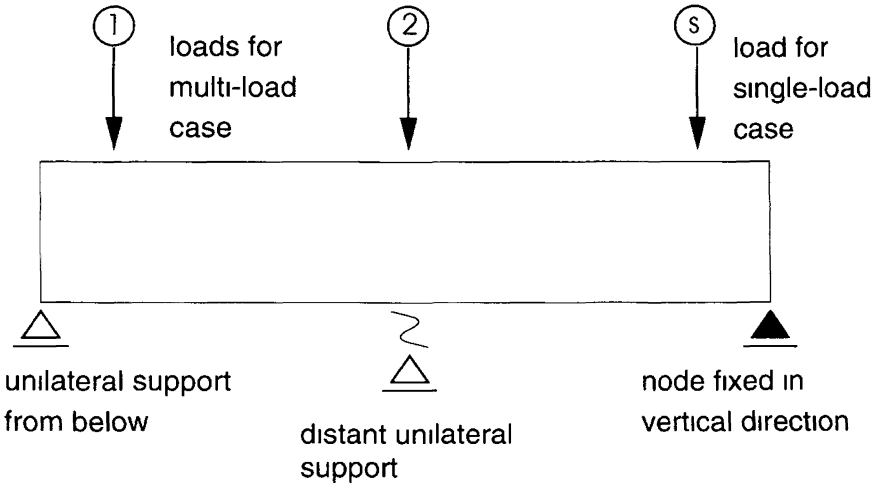

Figure 4. — Notation.

Figure 5(a) shows the optimal truss for multi load problem without considering contact, i e , the four supported nodes are *fixed* in the vertical direction In the next four figures (b)-(e) we consider unilateral contact conditions First we present a solution when we collect all the forces into one load-case (*figure* 5(b)) It resembles the previous design and uses, in fact, all the supporting nodes The next figures (c) and (d) show optimal designs for only one load-case the first and the second one, respectively Truss from figure (c) uses only the two outer supports, while the truss on figure (d), apparently, only the two inner supports Finally, figure 5(e) shows an optimal truss for the full multi-load contact problem It is a kind of reinforcement of the truss from figure (c) and uses the two outer supports in the first load-case and the inner supports in the second load-case A comparison of (a) and (e) shows how much is the optimal structure influenced by the different (bilateral and unilateral) contact conditions

Example 2 Now we take a truss of length height 5×1, again with 17×7 nodes and 4322 potential bars, and support it from below by two supports at the lower corners and one distant support for the lower middle node Needless to say, this situation cannot be simulated by classical (bilateral) boundary conditions, in principal Again, we have two load-cases, as depicted in figure 6(b) In figure 6(a) we collect the two forces in one load case, while figure 6(b) presents the result for the general multi-load contact problem

3. THE CONTINUUM CASE. MATERIAL OPTIMIZATION

In this chapter we study the case of a *continuum* structure There are two tracks one can follow either we work with *one* material and ask how to distribute this material in space, or we consider the material itself as *a function of the space variable x* The first approach is the direct extension of the discrete truss problem from Chapter 2 It is known, however, that the infinite-dimensional pendants of (2 8) and (2 9) may have no solutions in the sense of a 0/1 distribution of one given material They way out of this difficulty is to introduce the concept of *relaxation* which has been developed over the recent years (see, e g [4, 11])

We will follow the second track of variable material, which at a first glance looks more complex but it is not The question possesses an answer in the enlarged design space and it is numerically tractable after some analysis which reduces the unknown design *matrix function* $E(\ .\ )$ to the *trace* of E as unknown After a standard finite element discretization, we end up with a problem of form (2 8) where the role of the design vector t is now played by the trace of E Then the way is open for our software developed for the discrete truss case

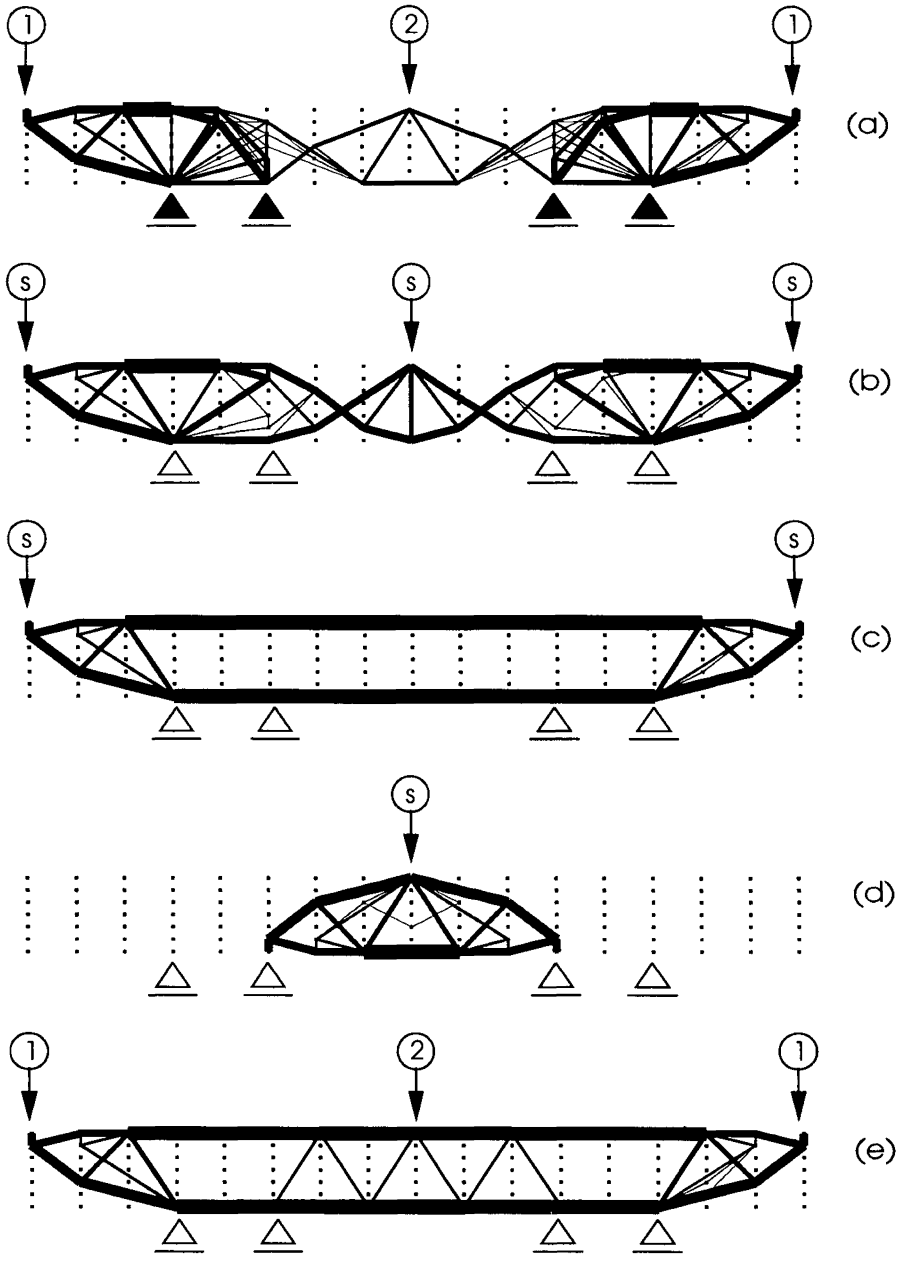

Figure 5. — Results for Example 1.

The idea to treat the material as a function of the space variable x goes back to Bendsøe *et al.* [10]. We follow their proposal and sketch only in short the problem formulation, the existence of a solution in the infinite-dimensional setting and the mathematical steps which lead to a discretized version of form (2.8).

In order to avoid a too heavy notation, we study the problem in $\mathbb{R}^2$ and deal with the single-load case only. Everything carries over immediately to $\mathbb{R}^3$.

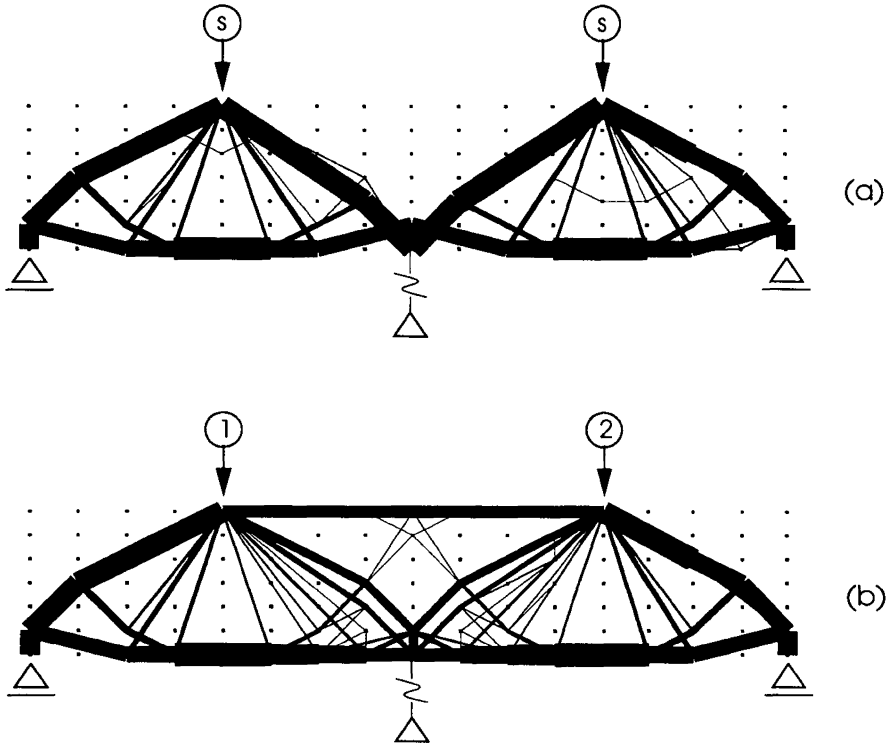

Figure 6. — Results for Example 2.

3.1. The single-load problem with contact: problem formulation

Throughout the following, let $\Omega \subset \mathbb{R}^2$ be a bounded domain with a Lipschitz boundary Γ. We use the standard notation $[H^1(\Omega)]^2$ and $[H_0^1(\Omega)]^2$ for Sobolev spaces of functions $u : \Omega \to \mathbb{R}^2$.

By $u = (u_1, u_2) \in [H^1(\Omega)]^2$ we denote the *displacement vector*, by $e_{ij}(u) = \frac{1}{2}\left(\frac{\partial u_i}{\partial x_j} + \frac{\partial u_j}{\partial x_i}\right)$ for $i, j = 1, 2$ the *(small-)strain tensor* and by $\sigma_{ij}(i, j = 1, 2)$ the *stress tensor*. Just as in Chapter 2, we assume that our system is governed by the linear Hooke's law, i.e., the stress is a linear function of the strain

$$\sigma = Ee \quad (\text{in tensor notation } \sigma_{ij} = E_{ijk\ell}\, e_{k\ell}),$$

where E is the so-called (plain-stress) *elasticity* tensor of order 4. In our context, it will be convenient to interpret the symmetric 2-tensors e and σ as vectors

$$e = (e_{11}, e_{22}, e_{12})^T \in \mathbb{R}^3, \quad \sigma = (\sigma_{11}, \sigma_{22}, \sigma_{12})^T \in \mathbb{R}^3$$

and, correspondingly, the 4-tensor E as a symmetric 3×3 matrix

$$E = \begin{pmatrix} E_{1111} & E_{1122} & E_{1112} \\ & E_{2222} & E_{2212} \\ \text{sym.} & & E_{1212} \end{pmatrix}.$$

We stress once more that in our approach not only e and σ but also E is a function of the space variable x; to emphasize this, we will sometimes write $E(\,.\,)$ instead of E. To include the 0/1-case of material/no-material, it is natural to work with

$$E \in [L^\infty(\Omega)]^{3\times 3} \quad (\text{in short: } E \in L^\infty(\Omega)).$$

Just as in the discrete case we assume that our elastic body is in frictionless unilateral contact with a rigid obstacle. Assume that the obstacle can be described by a function $\varphi \in C^0(\mathbb{R})$ in a local coordinate system (ξ_1, ξ_2). A typical situation is depicted in figure 7. We locate the system (ξ_1, ξ_2) such that ξ_1 is normal and ξ_2 tangential to Γ at some point P in the expected contact part of the boundary locally described by a Lipschitz function $\psi \in C^{0,1}(\mathbb{R})$:

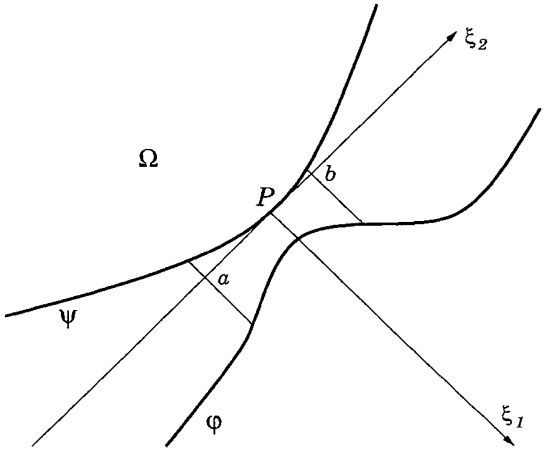

Figure 7. — Local coordinate system for the obstacle φ.

$$\Gamma_c = \{(\xi_1, \xi_2) \in \Gamma \,|\, a \leqslant \xi_2 \leqslant b,\ \xi_1 = \psi(\xi_2)\}. \tag{3.1}$$

The contact (non-penetration) condition is then:

$$u_{\xi_1} \leqslant \psi(\xi_2) - \varphi(\xi_2) \quad \text{for all } \xi_2 \in [a, b]$$

where u_{ξ_1} is the displacement in the direction of ξ_1.

We consider the partitioning of the boundary Γ into three parts: $\Gamma = \bar{\Gamma}_1 \cup \bar{\Gamma}_2 \cup \Gamma_c$, where Γ_1, Γ_2 and Γ_c are open in Γ and $\Gamma_2 \cap \Gamma_c = \phi$. Further we put $\mathscr{H} = \{u \in [H^1(\Omega)]^2 \,|\, u_i = 0 \text{ on } \Gamma_1 \text{ for } i = 1 \text{ or } 2 \text{ or for both}\}$, i.e., $[H_0^1(\Omega)]^2 \subset \mathscr{H} \subset [H^1(\Omega)]^2$.

Finally, we define the set of admissible displacements as

$$K := \{u \in \mathscr{H} \,|\, u_{\xi_1} \leqslant \psi(\xi_2) - \varphi(\xi_2) \text{ for all } \xi_2 \in [a, b]\}. \tag{3.2}$$

To exclude rigid-body displacements, we assume in the rest of this chapter that the set

$$\{v \in K | v_1 = a_1 + bx_1,\ v_2 = a_2 + bx_2,\ a_1, a_2 \in \mathbb{R},\ b \in \mathbb{R} \text{ arbitrary}\}$$

is empty.

For the elasticity tensor E and a given external load function $f \in [L_2(\Gamma_2)]^2$, the potential energy of an elastic body as a function of the displacement function u is given by (compare (2.2) for the discrete case)

$$\Pi(E, u) = \int_\Omega \frac{1}{2} \langle E(x)\, e(u(x)), e(u(x)) \rangle\, dx - \int_{\Gamma_2} f(x) \cdot u(x)\, dx .$$

The system is in equilibrium for u which minimizes the potential energy over the admissible set, i.e.,

$$\min_{u \in K} \Pi(E, u) .$$

Now the goal of the designer consists in finding some matrix function $E(\,\cdot\,)$ under suitable constraints such that the above 'min' is as big as possible. Physics tells us that the elasticity matrix has to be *symmetric* and *positive semidefinite* on all of Ω, what we write as

$$E(x) \geqslant 0 \quad \text{for all } x \in \Omega \quad (\text{or, in short: } E \geqslant 0) .$$

To exclude trivial solutions (the 'best' material is of stiffness 'infinity' for all $x \in \Omega$) we introduce the trace of E as a *cost function*

$$\operatorname{tr} E(x) = E_{1111}(x) + E_{2222}(x) + E_{1212}(x)$$

and consider only E with

$$\int_\Omega \operatorname{tr} E(x)\, dx \leqslant V$$

for some positive V. From $E \geqslant 0$ we know that $\operatorname{tr} E(x) \geqslant 0$ for all $x \in \Omega$ and, to exclude singularities, we further require with some $\bar{t} > 0$

$$0 \leqslant \operatorname{tr} E(x) \leqslant \bar{t} \quad \text{for all } x \in \Omega .$$

Thus, in mathematical language, our design problem becomes

$$\max_{\substack{E \in L^\infty(\Omega) \\ E \geqslant 0,\ \int_\Omega \operatorname{tr} E\, dx \leqslant V \\ 0 \leqslant \operatorname{tr} E \leqslant \bar{t}}} \ \min_{u \in K} \Pi(E, u) . \tag{3.3}$$

The existence of an optimal solution follows from a well-known saddle-point argument (see, e.g., [12], [14]).

THEOREM 5: *Problem (3.3) has an optimal solution* $(E^*, u^*) \in L^\infty(\Omega) \times K$.

Proof: Any saddle-point of (3.3) is a solution of (3.3). The existence of such a saddle-point follows from [12] if we can guarantee that

(i) $\Pi(\,\cdot\,, u) : L^\infty(\Omega) \to \mathbb{R}$ is concave and continuous in the weak*-topology for each fixed $u \in K$;

(ii) $\Pi(E, \,\cdot\,) : K \to \mathbb{R}$ is convex and continuous in the topology of $[H^1(\Omega)]^2$ for each fixed $E \in L^\infty(\Omega)$, $E \geqslant 0$;

(iii) the set $\mathscr{P} := \left\{ E \in L^\infty(\Omega) \,|\, E \geq 0, \int \operatorname{tr} E \, dx \leq V \right\} \subset L^\infty(\Omega)$ is convex and weak*-compact;

(iv) $\Pi(E^0, u)$ is coercive on K in u for suitable E^0.

Conditions (i) and (ii) hold trivially. From $E \geq 0$ and $0 \leq \operatorname{tr} E \leq \bar{t}$ it easily follows that $E \in \mathscr{P}$ lies in a norm ball of $L^\infty(\Omega)$ which implies the weak*-compactness of $\mathscr{P}$ and thus (iii). Finally, the proof of (iv) is somewhat more techical; it is based on the Korn's inequality and can be found, e.g., in [16, Theorem 2.2.5]. ■

3.2. Analytic reduction of $E(\,.\,)$ to trace of $E(\,.\,)$

Given the existence of an optimal E^*, we ask how to 'compute' this matrix function E^*. The crucial step lies in a clever reformulation of (3.3), which allows a partial analytic maximization with respect to E and leaves us with a maximum-problem in u and the trace of E as unknowns.

We start with a technical result. Note that the auxiliary function $\rho \in L^\infty(\Omega)$ in (3.4) is only a scalar function.

PROPOSITION 6: *It holds that*

$$\max_{\substack{E \in L^\infty, E \geq 0 \\ \int_\Omega \operatorname{tr} E \, dx \leq V \\ 0 \leq \operatorname{tr} E \leq \bar{t}}} \min_{u \in K} \Pi(E, u) = \max_{\substack{\rho \in L^\infty \\ \int_\Omega \rho \, dx \leq V \\ 0 \leq \rho \leq \bar{t}}} \min_{u \in K} \left\{ \int_\Omega \left[\max_{\substack{E(x) \geq 0 \\ \operatorname{tr} E(x) = \rho(x)}} \frac{1}{2} \langle E e(u), e(u) \rangle \right] dx + \int_{\Gamma_2} f \,.\, u \, dx \right\}. \tag{3.4}$$

Proof: With $\rho \in L^\infty(\Omega)$ we can split the 'max' in (3.3) as follows:

$$(3.3) = \max_{\substack{\rho \in L^\infty \\ \int_\Omega \rho \, dx \leq V \\ 0 \leq \rho \leq \bar{t}}} \max_{\substack{E \geq 0 \\ \operatorname{tr} E = \rho}} \min_{u \in K} \Pi(E, u) \,.$$

Here we use the fact that the absolute value of an off-diagonal element m_{ij} of a symmetric positive definite matrix M is bounded from above by $\sqrt{m_{ii} m_{jj}}$, hence the condition $E \in L^\infty$, $E \geq 0$ can be replaced by $\operatorname{tr} E \in L^\infty$, $E \geq 0$. Items (i)-(iii) in the proof of Theorem 6 tell us that we can switch the inner 'max-min' in the last expression:

$$(3.3) = \max_{\substack{\rho \in L^\infty \\ \int_\Omega \rho \, dx \leq V \\ 0 \leq \rho \leq \bar{t}}} \min_{u \in K} \max_{\substack{E \geq 0 \\ \operatorname{tr} E = \rho}} \Pi(E, u) \,.$$

The constraints on E under the inner 'max' are of *local nature* only (the *global part* '$\int \rho \, dx \leq V$' is separated and assigned to the outer 'max') and thus we can put the inner 'max' under the integral and compute $E(x)$ pointwise; this proves the claim. ■

We use standard LP theory to 'compute' the $E(x)$ under the integral in (3.4) for each fixed $x \in \Omega$.

THEOREM 7: *Fix $u \in K$ and $\rho \in L^\infty(\Omega)$ in (3.4). Then the maximizing $E_{\text{opt}}^{\rho, u}$ under the integral as a function of ρ and u becomes*

$$E_{\text{opt}}^{\rho, u}(x) = \rho \frac{1}{\operatorname{tr} \left[e(u(x)) \, e(u(x))^T \right]} e(u(x)) \, e(u(x))^T. \tag{3.5}$$

Proof For each fixed $x \in \Omega$, the 'max' under the integral in (3 4) is a function of $E(x)$ only (we skip the x)

$$\max_{\substack{E \geq 0 \\ \operatorname{tr} E = \rho}} \frac{1}{2} e^T E e \tag{3 6}$$

This is a linear program on the cone of symmetric positive semidefinite matrices The extremal rays of this cone are the dyadic products and thus $E^{\rho u}_{\text{opt}}$ must be of the form bb^T for a suitable $b \in \mathbb{R}^3$ Hence in (3 6) we essentially maximize the term

$$e^T E e = (e^T b)^2$$

with respect to b and the maximum will be obtained for $b = \alpha e$ with $\alpha \geq 0$ A second look at the constraints in (3 6) yields

$$E^{\rho u}_{\text{opt}} = \rho \frac{1}{\operatorname{tr}[ee^T]} ee^T$$

■

Remark For a fixed $x \in \Omega$, let us change the coordinate system such that the new coordinates coalign with the main strain directions denoted by $e_1(x)$, $e_2(x)$ (Recall that the main strain directions are the (orthogonal) eigenvectors of the matrix $\begin{pmatrix} e_{11} & e_{12} \\ e_{21} & e_{22} \end{pmatrix}$) Hence, in the new coordinate system, the optimal material matrix is given by

$$E^{\rho u}_{opt} = \rho \frac{1}{e_1^2 + e_2^2} \begin{pmatrix} e_1 \\ e_2 \\ 0 \end{pmatrix} (e_1, e_2, 0)^T = \begin{pmatrix} \rho \dfrac{e_1^2}{e_1^2 + e_2^2} & \rho \dfrac{e_1 e_2}{e_1^2 + e_2^2} & 0 \\ \rho \dfrac{e_1 e_2}{e_1^2 + e_2^2} & \rho \dfrac{e_2^2}{e_1^2 + e_2^2} & 0 \\ 0 & 0 & 0 \end{pmatrix} \tag{3 7}$$

The optimal material (3 7) is orthotropic and has zero shearing stiffness Thus the material can only carry strain fields which are rescalings of the given strain field for which the optimization was undertaken

By inserting (3 5) into (3 4) and noting that $\operatorname{tr}[ee^T] = e^T e$, we end up with

THEOREM 8 *The optimal material problem (3 3) reduces to*

$$(3\,3) = \max_{\substack{\rho \in L^\infty(\Omega) \\ \int_\Omega \rho(x)\,dx \leq V \\ 0 \leq \rho \leq t}} \min_{u \in K} \left\{ \int_\Omega \left[\frac{1}{2} \rho(x) \langle e(u(x)), e(u(x)) \rangle \right] dx - \int_{\Gamma_2} f(x) \cdot u(x)\, dx \right\} \tag{3 8}$$

This problem has an optimal solution (ρ^*, u^*) *from which an optimal* E^* *can be recovered according to (3 5)*

Proof The existence of an optimal solution (ρ^*, u^*) follows just as in the proof of Theorem 6 The rest is obvious ■

3.3. Discretized problem

So far, our considerations were carried out in an infinite-dimensional context. To be able to solve (3.8) numerically, we have to discretize it. For the discretization we use the finite element method. At this point we remark, that our reduced problem (3.8) is a special case of the so-called variable-thickness sheet problem

$$\max_{\substack{\rho \in L^\infty(\Omega) \\ \int_\Omega h(x)\,dx \leq V \\ 0 \leq h \leq \bar{t}}} \min_{u \in K} \left\{ \int_\Omega \left[\frac{1}{2} h(x) \langle E(x)\, e(u(x)), e(u(x)) \rangle \right] dx - \int_{\Gamma_2} f(x) \cdot u(x)\, dx \right\}. \tag{3.9}$$

with *fixed* material properties and variable thickness $h \in L^\infty(\Omega)$. Hence we can use the convergence theory developed for (3.9) in [22] to guarantee convergence of solutions to the discrete problems defined below towards the solution of (3.8). Since this is not the main goal of this paper, we do not repeat here the details of this analysis and only show how to reach the discrete version of (3.8).

To simplify the notations, we use the same symbols for the discrete objects (vectors) as for the 'continuum' ones (function). Assume that Ω can be partitioned into m squares (elements) Ω_i, $i = 1, ..., m$ of the same dimension (otherwise we use the standard isoparametric concept, *cf.* [13]). Let us denote by n the number of nodes (vertices of the squares). Assume that $\rho(x)$ is approximated by a function that is constant on each element, i.e., it is fully characterized by a vector $\rho = (\rho_1, ..., \rho_m)$ of its element values. Further assume that the displacement vector $u(x)$ is approximated by a continuous function that is bi-linear (linear in each coordinate) on every element. Such a function can be written as

$$u(x) = \sum_{i=1}^{n} u_i\, \vartheta_i(x)$$

where u_i is the value of u at i^{th} node and ϑ_i is the basis function associated with i^{th} node (for details, see [13]). Recall that, at each node, the displacement has two components, so $u \in \mathbb{R}^{2n}$. For discussion on higher-order finite-element approximation and the relation to so-called checkerboard phenomenon, see [11].

Further we define the discrete version of the set K of admissible displacements. Let v be the vector of direction cosines of the local coordinate ξ_2 (*cf.* (3.1)) and C_i the $(n \times 2n)$ matrix that picks up from the displacements vector u the two components associated with node number i. Also, let $g \in \mathbb{R}^r$ be the vector of the gaps $\psi(\xi_2) - \varphi(\xi_2)$ at r nodes of the discretized boundary Γ_c. With an $r \times 2n$ matrix

$$C := -\begin{pmatrix} v^T C_1 \\ \vdots \\ v^T C_r \end{pmatrix},$$

defined for the contact boundary nodes, the discrete admissible set (3.2) takes the form

$$K := \{ u \in \mathbb{R}^{2n} \mid Cu \leq g \}. \tag{3.10}$$

For basis functions ϑ_k, $k = 1, ..., n$, we define matrices

$$B_k = \begin{pmatrix} \dfrac{\partial \vartheta_k}{\partial x_1} & 0 \\ 0 & \dfrac{\partial \vartheta_k}{\partial x_2} \\ \dfrac{1}{2}\dfrac{\partial \vartheta_k}{\partial x_2} & \dfrac{1}{2}\dfrac{\partial \vartheta_k}{\partial x_1} \end{pmatrix}.$$

Now, for an element Ω_i, let $\mathscr{D}_i$ be an index set of nodes belonging to this element. With

$$A_i = \sum_{k,\, \ell \in \mathscr{D}_i} \int_{\Omega_i} B_k^T B_\ell \, dx$$

being the element stiffness matrix and f the discretized right-hand side, the discrete version of (3.8) takes the form:

$$\max_{\substack{\rho \geq 0 \\ \sum \rho_i \leq mV}} \min_{u \in K} \left[\frac{1}{2} u^T \left(\sum_{i=1}^{m} \rho_i A_i \right) u - f^T u \right]. \tag{3.11}$$

Here the constraint on resources $\int_\Omega \rho \, dx \leq V$ is replaced by $\sum \rho_i \leq mV$; further we assume that $\bar{t} \geq mV$ and skip the constraint $\rho \leq \bar{t}$. (The latter only works for 'finite' values of m; for the asymptotic analysis, one would have to use a refined technique in the following, *cf.* [6].)

In the final step, we eliminate the variable ρ (analogously to the truss problem with variable t). Using again the Minimax Theorem [27], we write (3.11) as

$$\min_{u \in K} \max_{\substack{\rho \geq 0 \\ \sum \rho_i \leq mV}} \left(\frac{1}{2} u^T A_1 u - f^T u, \ldots, \frac{1}{2} u^T A_m u - f^T u \right) \begin{pmatrix} \rho_1 \\ \vdots \\ \rho_m \end{pmatrix}$$

and, following steps (2.13) $\rightarrow$ (2.15) $\rightarrow$ (2.16), we arrive at the formulation

$$\underset{u \in K,\, \alpha \in \mathbb{R}}{\text{minimize}} \; -\alpha - f^T u \quad \text{subject to} \quad \frac{mV}{2} u^T A_i u \leq -\alpha, \quad i = 1, 2, \ldots, m \tag{3.12}$$

which is exactly the same as the truss optimization problem (2.16) (m is a fixed parameter, so we can replace mV by $\tilde{V} = mV$). Thus we can use the same optimization software, where only the part for generating the stiffness matrices A_i differs. However, the character of these matrices is different from the truss design problem: the global matrix $\sum_{i=1}^{m} A_i$ is sparse now. To exploit this sparsity, in the Newton method we implemented a sparse skyline solver for systems of linear equations (*cf.*, e.g. [5]).

3.4. Examples

Results for two numerical examples are presented in this section. The values of the 'density' function ρ are depicted by gradations of grey: full black corresponds to high density, etc. We only consider single-load problems.

Example 3: The first example is analogous to the single-load truss problem from Example 2 (*cf. fig.* 6(a)). Figure 8 shows the optimal material distribution (the values of function ρ) for the discretization by 61×13 elements. Also shown are the directions and magnitudes of the principal stresses in the particular elements.

Example 4: This example is taken from [24] to show the differences between our approach and the variable-thickness sheet optimization. The geometry, forces and boundary conditions are shown in figure 9. The function that determines the gap between the body and the obstacle is defined as

$$6.4 \cdot x_1^4$$

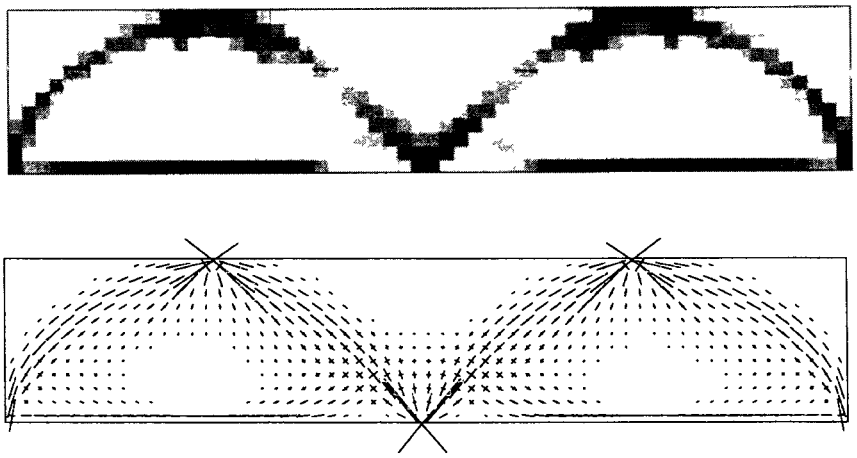

Figure 8. — Example 3, optimal distribution of ρ, direction and magnitude of optimal principal stress.

with the origin at the left-lower corner, and symmetrically for the right-lower corner. The upper part (boundary Γ_1) is fixed in *both* directions. We first show a result for the problem *without* obstacles. It is depicted in figure 10 and is 'surprisingly' simple. The optimal material has zero stiffness outside the black region (that means, there is no material there) and is only vertically stiff (and homogeneous) inside it. The optimal elasticity matrix inside the black region reads as

$$\begin{pmatrix} 0 & 0 & 0 \\ 0 & E_{2222} & 0 \\ 0 & 0 & 0 \end{pmatrix}.$$

The material consists here of infinitesimally many infinitesimally thin fibres. This result is in contrast to that for the variable-thickness sheet problem where, due to nonzero Poisson ratio, the body is wider and wider as it approaches the upper fixed boundary. (The conclusion is that one should be careful about which approach to choose for topology optimization.)

Now let us return to the contact problem. The optimal material distribution for the example from figure 9 is shown in figure 11. The optimized body partly uses the obstacle and partly the fixed part of the boundary to carry the load. Figure 11 shows also the directions and magnitudes of principal stresses in the finite elements.

4. THE PENALTY/BARRIER MULTIPLIERS (PBM) METHOD

In this section we present the PBM method [8], [9] which we used in our numerical computations. This chapter is rather self-contained and we use here the standard notation from Mathematical Programming, e.g., f for the objective function, etc. So at this moment, the reader should forget the notation from the rest of the paper; we hope that this is not too confusing.

PBM proved to be a very efficient tool for solving problems (2.16), (3.12) and, in general, large scale *nonlinear programs* of the type

$$(P) \quad \min_{x \in \mathbb{R}^n} \{f(x) : g_i(x) \leq 0\}, \quad i = 1, ..., m$$

where f and g_i are nonlinear functions.

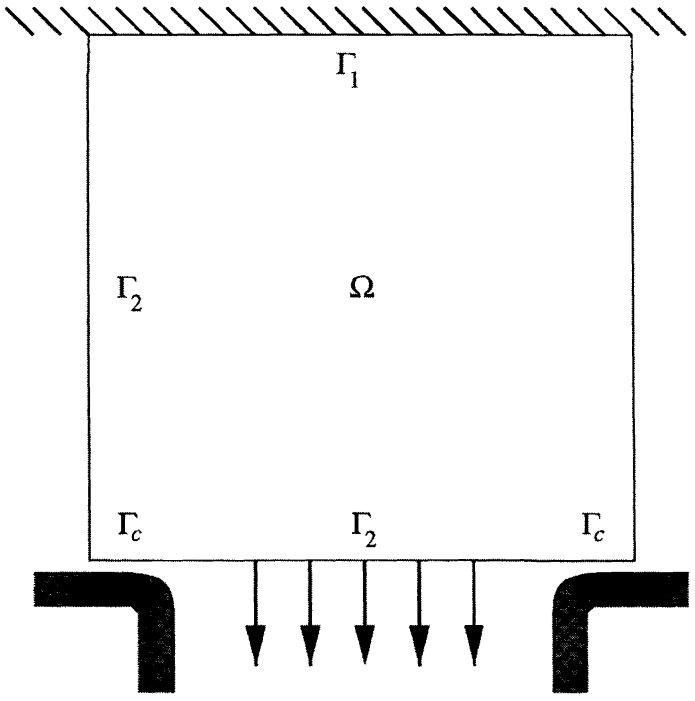

Figure 9. — Example 4.

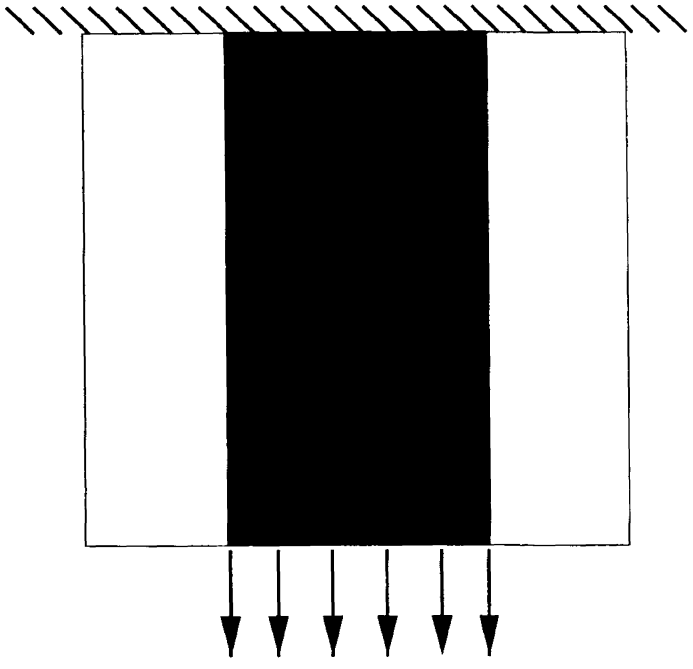

Figure 10. — Example 4 without contact, optimal distribution of ρ

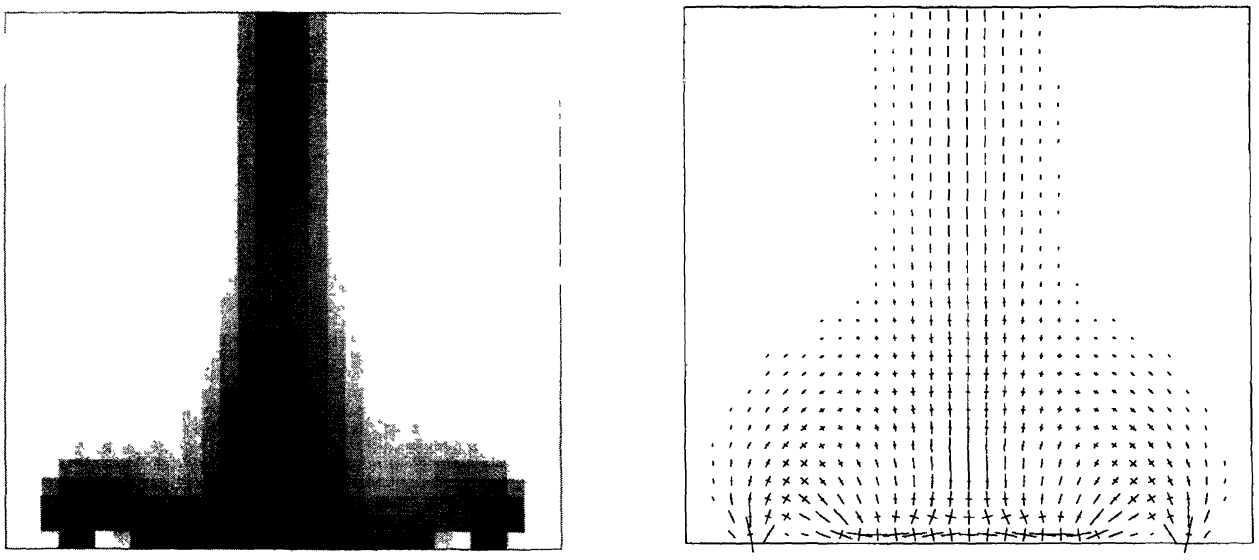

Figure 11. — Example 4, optimal distribution of ρ; direction and magnitude of optimal principal stress.

The *classical Lagrangian* of the problem (P) is the function $L: \mathbb{R}^n \times \mathbb{R}^m_+ \to \mathbb{R}$ given by

$$L(x, \lambda) = f(x) + \sum_{i=1}^{m} \lambda_i g_i(x) . \tag{4.1}$$

We transform the constraints of problem (P) using an increasing twice differentiable, real-valued convex function φ, with $\operatorname{dom} \varphi = (-\infty, b)$, $0 < b \leqslant \infty$ which, in addition, has the following properties:

$$(\varphi 1) \quad \varphi(0) = 0$$

$$(\varphi 2) \quad \varphi'(0) = 1$$

$$(\varphi 3) \quad \lim_{\tau \to b} \varphi'(\tau) = \infty$$

$$(\varphi 4) \quad \lim_{\tau \to -\infty} \varphi'(\tau) = 0$$

$$(\varphi 5) \quad \varphi''(\tau) \geqslant \frac{1}{M} \text{ for all } 0 \leqslant \tau \leqslant b, \text{ for some } M > 0 .$$

Let p be a positive number; then the function $p\varphi(\tau/p)$ has the same properties as φ and, in particular,

$$p\varphi(\tau/p) \leqslant 0 \quad \text{if and only if} \quad \tau \leqslant 0 .$$

Consequently, the constraints in problem (P) can be equivalently replaced by

$$p_i \varphi(g_i(x)/p_i) \leqslant 0, \quad i = 1, \ldots, m \tag{4.2}$$

where $p_i > 0$ is a *penalty parameter* for the i-th constraint. The Lagrangian corresponding to minimizing $f(x)$ subject to the constraints (4.2) is

$$\mathscr{L}(x, \lambda, p) = f(x) + \sum_{i=1}^{m} \lambda_i p_i \varphi(g_i(x)/p_i) . \tag{4.3}$$

We call this $\mathscr{L}$ *augmented Lagrangian* for problem (P). It is easily verified, using the properties of φ, that a pair $(x^*, \lambda^*) \in \mathbb{R}^n \times \mathbb{R}^m_+$ is a saddle point of the Lagrangian (4.1) if and only if it is a saddle point of the augmented Lagrangian (4.3).

The methods from the PBM family are iterative. At each iteration we minimize the augmented Lagrangian with respect ot x

$$x^{k+1} = \arg\min_x \mathscr{L}(x, \lambda^k, p^k) \tag{4.4}$$

and update the multipliers and the penalty parameter:

$$\lambda_i^{k+1} = \lambda_i^k \varphi'(g_i(x^{k+1})/p^k) \tag{4.5}$$

$$p^{k+1} = \pi p^k . \tag{4.6}$$

Here π is a *penalty updating factor.* A specific algorithm in the PBM family is determined by the particular choice of the function φ.

The updating of multipliers (4.5) is motivated by the optimality condition at x^{k+1} (see (4.4))

$$0 = f'(x^{k+1}) + \sum \lambda_i^k \varphi'(g_i(x^{k+1})/p^k)\, g_i'(x^{k+1}) .$$

Choosing λ^{k+1} by (4.5), we further get

$$0 = f'(x^{k+1}) + \sum \lambda_i^{k+1} g_i'(x^{k+1}) = L_x'(x^{k+1}, \lambda^{k+1}) .$$

Thus, for this choice of λ^{k+1}, x^{k+1} is a minimizer of the *classical* Lagrangian (4.1). Moreover, a lower bound for the optimal value of (P) is produced by the dual objective function:

$$f(x^*) \geqslant G(\lambda^{k+1}) =: \min_x L(x, \lambda^{k+1}) = L(x^{k+1}, \lambda^{k+1}) .$$

The updating formula (4.5) can be explained more intuitively as follows: if x^{k+1} is outside of the feasible set with respect to thc i-th constraint $(g_i(x^{k+1}) > 0)$ then the influence of this constraint grows since its multiplier λ_i^k is increased (recall that by property $(\varphi 2)$, $\varphi'(g_i/p_i^k) > 1$ for positive g_i; hence $\lambda_i^{k+1} > \lambda_i^k$).

Now we discuss examples of the function φ which give rise to some well-known multiplier methods.

1. **The Classical Quadratic Augmented Lagrangian** [26] is obtained by choosing

$$\varphi(\tau) = \begin{cases} \tau + \frac{1}{2}\tau^2, & \tau \geqslant -1 \\ -\frac{1}{2}, & \tau \geqslant -1 . \end{cases}$$

The quadratic branch has a smooth continuation by a constant, but the second derivative jumps at the joint, causing difficulties in using the Newton method for the minimization of $\mathscr{L}(x, \lambda^k, p^k)$.

2. **The Exponential Method of Multipliers** [28]
Here

$$\varphi(\tau) = e^{\tau} - 1 .$$

3. **Modified Barrier Method** [25]
Here φ is a shifted logarithmic function:

$$\varphi(\tau) = -\log(1 - \tau), \quad -\infty < \tau < 1 .$$

In examples 2 and 3, the second derivative of φ is continuous, but the third derivative is very large for certain values of τ, again causing difficulties to the Newton method.

In the next example, we present a "mixed quadratic-logarithmic" penalty function φ, which will give rise to our preferred (and implemented) multiplier method:

4. **Quadratic-Logarithmic PBM Method** [8] [9]

We set

$$\varphi_{\hat{\tau}}(\tau) = \begin{cases} i\,\frac{a}{2}\tau^2 + b\tau + c & \tau \geqslant \hat{\tau} \\ d\log(\tau - e) + f & \tau < \hat{\tau} \end{cases}$$

where $-1 < \hat{\tau} \leqslant 1$ is a parameter fixing the joint point. The coefficients a, b, c, d, e, f are uniquely determined by the requirement that φ is twice differentiable at $\tau = \hat{\tau}$, and $\varphi(0) = 0$, $\varphi'(0) = 1$, $\varphi''(0) = 1$. For example, if $-1 < \hat{\tau} \leqslant 0$ then

$$\varphi_{\hat{\tau}}(\tau) = \begin{cases} \tau + \frac{1}{2}\tau^2 & \tau \geqslant \hat{\tau} \\ -(1+\hat{\tau})^2 \log\left(\frac{1+2\hat{\tau}-\tau}{1+\hat{\tau}}\right) + \hat{\tau} + \frac{1}{2}\hat{\tau}^2 & \tau < \hat{\tau}\,. \end{cases} \tag{4.7}$$

We usually set $\hat{\tau} = -\frac{1}{2}$, as for this choice $e = 0$ and we get a pure (not shifted) logarithmic branch. This function combines, in a sense, the advantages of the interior logarithmic penalty function underlying recent *interior-point polynomial-time algorithms,* and those of external penalty, thus allowing to avoid serious computational difficulties arising in pure interior-point methods when they come close to the boundary of the feasible domain. Now *the second derivative φ'' is continuous and bounded for all $\tau \in \mathbb{R}$*; this is advantageous when we perform minimization step (4.4) of the algorithm by the modified Newton method with linesearch. Our choice of the logarithmic-quadratic penalty function (4.7) usually reduces the number of Newton steps 2-3 times, compared to the pure (shifted) logarithmic penalty, particularly for large-scale problems. Also, the linesearch needs much less function and gradient evaluations (typically only 2-3). Moreover, the method is less sensitive to the choice of the initial point x^0 and of the penalty parameter reduction factor π. For all problems we tested, the factor $\pi = 0.3$ worked well (and this was not the case for other types of φ mentioned above). In our implementation initial values are: $p^0 = 1.0$ and $\lambda_i^0 = 0.01$.

We stop the unconstrained minimization in (4.4) as soon as either the decrease of the function (4.4) in one Newton step is less than αp, of the norm of gradient $\| \mathscr{L}'_x(x, \lambda^k) \| < \alpha$. Typically, $\alpha = 0.1$, but sometimes a less conservative strategy with $\alpha = 2$, and with a slower penalty parameter updating, yields better results.

Whenever the multipliers are updated, their relative change is restricted by a factor μ:

$$\mu \leqslant \lambda_i^{k+1} / \lambda_i^k \leqslant 1/\mu$$

(typically $\mu = 0.3$). This prevents a drastic change of the augmented Lagrangian, which could cause a large number of Newton steps in the next iteration. Also, it restricts the influence of inaccuracy in the minimization on the values of the new multipliers, and moreover, prevents them from approaching zero too early.

After the penalty parameter achieves some limit value (say, $10^{-3} - 10^{-6}$), we do not update it any more, and continue only with updating the multipliers.

Empirically, we observed a remarkable feature of the method: usually, after achieving accuracy of 4 or 5 digits in the objective function value, every additional iteration requires only one Newton step, adding typically a digit of accuracy. (An analogous fact was proved in [20] for the MBF method applied to Linear Programming.) Due to this property, the method is particularly efficient when high accuracy (up to 10-12 digits) is required.

ACKNOWLEDGEMENTS

We would like to thank Martin Bendsøe from the Technical University of Denmark and Alejandro Diaz from the Michigan State University for providing us with the graphical software and parts of the software for truss generation.

REFERENCES

[1] W. ACHTZIGER. Truss topology design under multiple loading. DFG Report 367, Math. Institut, Univ. of Bayreuth, 1992.

[2] W. ACHTZIGER. Minimax compliance truss topology subject to multiple loadings. In M. Bendsøe and C. Mota-Soares, editors, *Topology optimization of trusses,* pages 43-54. Kluwer Academic Press, Dortrecht, 1993.

[3] W. ACHTZIGER, A. BEN-TAL, M. BENDSØE and J. ZOWE. Equivalent displacement based formulations for maximum strength truss topology design. *IMPACT of Computing in Science and Engineering,* 4: 315-345, 1992.

[4] G. ALLAIRE and R. KOHN. Optimal design for minimum weight and compliance in plane stress using extremal microstructures. *European J. on Mechanics (A/Solids),* 12: 839-878, 1993.

[5] K. J. BATHE and E. L. WILSON. *Numerical Methods in Finite Element Analysis.* Prentice-Hall, Inc., Englewood Cliffs, New Jersey, 1976.

[6] A. BEN-TAL and M. BENDSØE. A new iterative method for optimal truss topology design. *SIAM J. Optimization,* 3: 322-358, 1993.

[7] A. BEN-TAL, M. BENDSØE and J. ZOWE. Optimization methods for truss geometry and topology design. *Structural Optimization,* 7: 141-159, 1994.

[8] A. BEN-TAL, I. YUZEFOVICH and M. ZIBULEVSKY. Penalty/barrier multiplier methods for minmax and constrained smooth convex programs. Research report 9/92, Optimization Laboratory, Technion-Israel Institute of Technology, Haifa, 1992.

[9] A. BEN-TAL and M. ZIBULEVSKY. Penalty/barrier multiplier methods: a new class of augmented lagrangian algorithms for large scale convex programming problems. *SIAM J. Optimization,* 7, 1997.

[10] M. BENDSØE, J. GUADES, R. HABER, P. PEDERSEN and J. TAYLOR. An analytical model to predict optimal material properties in the context of optimal structural design. *J. Applied Mechanics,* 61: 930-937, 1994.

[11] M. P. BENDSØE. *Optimization of Structural Topology, Shape and Material.* Springer-Verlag, Heidelberg, 1995.

[12] J. CEA. *Lectures on Optimization.* Springer-Verlag, Berlin, 1978.

[13] P. G. CIARLET. *The Finite Element Method for Elliptic Problems.* North-Holland, Amsterdam, New York, Oxford, 1978.

[14] I. EKELAND and R. TEMAM. *Convex Analysis and Variational Problems.* North-Holland, Amsterdam, 1976.

[15] E. J. HAUG and J. S. ARORA. *Applied Optimal Design.* Wiley, New York, 1979.

[16] I. HLAVÁČEK, J. HASLINGER, J. NEČAS and J. LOVÍŠEK. *Solution of Variational Inequalities in Mechanics.* Springer-Verlag, New-York, 1988.

[17] F. JARRE, M. KOČVARA and J. ZOWE. Interior point methods for mechanical design problems. *SIAM J. Optimization.* To appear.

[18] A. KLARBRING, J. PETERSSON and M. RÖNNQUIST. Truss topology optimization involving unilateral contact. *J. Optimization Theory and Applications,* 87, 1995.

[19] M. KOČVARA and J. ZOWE. How mathematics can help in design of mechanical structures. In D.F. Griffiths and G.A. Watson, eds., *Numerical Analysis 1995,* Longman, Harlow, 1996, pp. 76-93.

[20] J. PETERSSON. On stiffness maximization of variable thickness sheet with unilateral contact. *Quarterly of Applied Mathematics,* 54: 541-550, 1996.

[22] J. PETERSSON and J. HASLINGER. An approximation theory for optimum sheet in unilateral contact. *Quarterly of Applied Mathematics.* To appear.

[23] J. PETERSSON and A. KLARBRING. Saddle point approach to stiffness optimization of discrete structures including unilateral contact. *Control and Cybernetics,* 3: 461-479, 1994.

[24] J. PETERSSON and M. PATRIKSSON. Topology optimization of sheets in contact by a subgradient method. International Journal for Numerical Methods in Engineerings. To appear.

[25] R. POLYAK. Modified barrier functions: Theory and methods. *Mathematical Programming,* 54: 177-222, 1992.

[26] R. T. ROCKAFELLAR. A dual approach to solving nonlinear programming problems by unconstrained optimization. *Mathematical Programming,* 5: 354-373, 1973.

[27] R. T. ROCKAFELLAR. *Convex Analysis.* Princeton University Press, Princeton, New Jersey, 1970.

[28] P. TSENG and D. P. BERTSEKAS. On the convergence of the exponential multiplier method for convex programming. *Mathematical Programming,* 60: 1-19, 1993.